

# Acessos ao balanço de energia em larga escala com uso conjunto de parâmetros obtidos por sensoriamento remoto e grades de dados climáticos na região de crescimento agrícola do SEALBA

**Antônio Heriberto de Castro Teixeira**<sup>1</sup>; **Janice Freitas Leivas**<sup>3</sup>; **Celina Maki Takemura**<sup>3</sup>; **Edlene Aparecida Monteiro Garçon**<sup>4</sup>; **Inajá Francisco de Souza**<sup>1</sup>; **Ana Flávia Maria Santos Azevedo**<sup>2</sup>

<sup>1</sup>Professor. Universidade Federal de Sergipe. Aracaju, Sergipe; <sup>2</sup>Bolsista. Universidade Federal de Sergipe. Aracaju, Sergipe; <sup>3</sup>Pesquisadora. Embrapa Territorial. Campinas, São Paulo; <sup>4</sup>Analista. Embrapa Territorial. Campinas, São Paulo

## RESUMO

O algoritmo SAFER (*Simple Algorithm for Evapotranspiration Retrieving*) foi aplicado com imagens MODIS e grades de dados climáticos para o período de 2007 a 2021, objetivando-se a implementação de um sistema de monitoramento dos componentes do balanço de energia, nos biomas Mata Atlântica (MA) e Caatinga (CT), dentro da região de crescimento agrícola SEALBA, Nordeste do Brasil. Diferenças significativas na partição do saldo de radiação ( $R_n$ ) nos fluxos de calor latente ( $\lambda E$ ), sensível ( $H$ ) e no solo ( $G$ ), promoveram distintas condições de umidade na zona das raízes, representadas pela fração evaporativa [ $E_f = \lambda E / (R_n - G)$ ]. Considerando os dados históricos, os valores de  $R_n$  não apresentaram grandes significativas entre os biomas, com médias anuais de 9,40 e 9,50 MJ m<sup>-2</sup> d<sup>-1</sup>, para MA e CT, respectivamente. Entretanto, respectivamente para MA e CT, as médias anuais para  $\lambda E$  foram 5,10 MJ m<sup>-2</sup> d<sup>-1</sup> e 4,00 MJ m<sup>-2</sup> d<sup>-1</sup>; para  $H$  elas foram 3,80 MJ m<sup>-2</sup> d<sup>-1</sup> e 5,00 MJ m<sup>-2</sup> d<sup>-1</sup>; e para  $G$  elas fora 0,50 MJ m<sup>-2</sup> d<sup>-1</sup> e 0,40 MJ m<sup>-2</sup> d<sup>-1</sup>, produzindo valores médios para  $E_f$  de 0.60 e 0.50 for para os biomas MA e CT, respectivamente, evidenciando maiores níveis de umidade na zona das raízes para o primeiro bioma. Comparando os resultados da  $E_f$  para os últimos quatro anos na série de dados, pôde-se concluir que as condições de umidade na zona das raízes apresentam grandes variações ao longo dos anos em ambos os biomas. Essas análises são importantes para as políticas de recursos hídricos visto que elas mostram períodos e regiões viáveis para a agricultura dependente de chuvas, bem como necessidades de irrigação para a agricultura irrigada, permitindo um manejo racional de água na agricultura enquanto fornecem suporte para minimização dos conflitos hídricos com outros setores.

**PALAVRAS-CHAVE:** partição de energia; fração evapotranspirativa; Floresta Atlântica; Caatinga;

## INTRODUÇÃO

### INTRODUCTION

Climate and land-use changes affecting the energy balance components have been detected worldwide making geotechnologies powerful tools for monitoring these components, to subsidize policies for rational environmental management (Teixeira et al., 2017a, b, 2021). Understanding the effects of these changes is critical for ecological restoration (Zhang et al. 2021), demanding large-scale studies to support sustainable explorations of the natural resources (Almeida et al., 2023).

Accounting the energy balance components, the net radiation ( $R_n$ ) is the difference between incoming and outgoing energy fluxes of both short and long wavelengths, being partitioned into latent ( $\lambda E$ ), sensible ( $H$ ), and ground ( $G$ ) heat fluxes, and the magnitudes of these partitions are dependent on solar radiation levels and the root-zone moisture conditions. Quantifying  $\lambda E$  is outstanding, because it represents the energy used for evapotranspiration, which is the main water use from any agroecosystems. On one hand, although evapotranspiration is related to agricultural production, increases of its rates means less water availability for other water user. On the other hand, the magnitude of  $H$  may indicate warming or cooling conditions (Teixeira et al., 2017a, b, 2021). Teixeira et al. (2017b) showed that the replacement of natural vegetation in Southeast Brazil by sugarcane

reduced  $\lambda E$  and increases H, while when this replacement is with coffee, the opposite situation was verified, increasing  $\lambda E$  and dropping H. Quantifying these components is meaningful to assess the dimension of environmental impacts (Zhang et al., 2021).

In the coastal Brazilian biomes, inside the Northeast region, the ecosystems are experiencing environmental impacts because of deforestations; burnings; air, water and soil pollutions, as well intensive agricultural crops replacing the natural vegetation (Lewinsohn and Prado, 2005; Mariano et al., 2018). This is the case of SEALBA, acronym for the agricultural growing region involving the states of Sergipe (SE), Alagoas (AL) and Bahia (BA), with mixed agroecosystems within the Atlantic Forest (AF) and Caatinga (CT) biomes. These impacts demand large-scale energy balance studies to support the rational agricultural managements to minimize the consequences of these impacts. Agriculture in SEALBA has increased over the last years, and these land use changes, together climate alterations, affect the available energy partitions into  $\lambda E$  and H, what can increase water consumptions and warming conditions.

The delimitation of the agricultural potential for SEALBA was based on the average totals of precipitation ranging between 450 and 1400 mm, from April to September. According to Procópio et al. (2019), these rainfall amounts could supply water for several crops (grains, fruits, sugar cane, forestry, and pasture). However, to know the real water availabilities for agriculture, besides rainfall as input, the output, i.e., water fluxes represented here by  $\lambda E$  in energy units, must be also considered. In the SEALBA coastline, is the AF biome and more to the west side is the CT biome, both experiencing replacements of their natural vegetation by agricultural crops. Despite their aptitude for agriculture when water is available, this fast replacement, together with climate changes, can contributes to increase environmental impacts. The use of long-term energy balance data may be suitable for policy decision-making under these conditions.

Some field energy balance studies were done by different methods in the AF and CT biomes (Marques et al., 2020; Pereira et al., 2010; Silva et al., 2017; Teixeira et al., 2008). However, time specific point measurements are not suitable for large-scale long-term accountings, because of strong spatial and temporal variations on the energy exchanges between surfaces and the lower atmosphere. Few efforts have been carried out for monitoring the energy balance components along the years inside these biomes considering a long data series for average conditions. These analyzes can help to understand the responses of natural vegetation and agricultural crops to the negative environmental impacts.

Considering operational aspects of the Penman-Monteith equation was considered for elaboration of the SAFER (Simple Algorithm for Evapotranspiration Retrieving) algorithm, by using simultaneous field and remote sensing measurements in Northeast Brazil to estimate the energy balance components (Teixeira, 2010; Teixeira et al., 2008). The reason for the SAFER's choice in the current research, besides its applicability, other important advantage, regarding other algorithms, is that in its newer version there is no need of the thermal bands, being possible to use only the red and near infrared bands, more easily available (Consoli and Vanella, 2014). In addition, the thermal bands of the MODIS sensor used in the current research, having a spatial resolution of 1 km, means that the images should cover more mixed surface types, when comparing with the 250-m spatial resolution of its red and near infrared bands.

## **OBJETIVOS**

### **OBJECTIVES**

Aiming to implement an operational monitoring system for biomes experiencing climate and land-use changes, taking the SEALBA region as a reference, we tested the latest version of the SAFER algorithm, by using MODIS MOD13Q1 reflectance products and long-term weather data from 2007 to 2021 at the same satellite 16-day timescales, to retrieve the dynamic of the energy balance

components along the years. The authors believe that the success of applications for this specific region within Northeast Brazil may encourage replications of the methods in other environmental conditions with probably simple calibrations of the modelling equations.

## MATERIAL E MÉTODOS

### MATERIAL AND METHODS

#### Biomes and data set

Figure 1 shows the location of the SEALBA agricultural growing region within the Brazilian states of Sergipe - SE, Alagoas - AL, and Bahia - BA, in Northeast Brazil (Figure 1a); biomes involved by the region (Figure 1b) according to the Geographic and Statistical Brazilian Institute (IBGE. [www.ibge.gov.br](http://www.ibge.gov.br)); and altitudes together with the 17 weather stations used (Figure 1c) from the National Meteorological Institute (INMET. <https://www.gov.br/agricultura/pt-br/assuntos/inmet>).

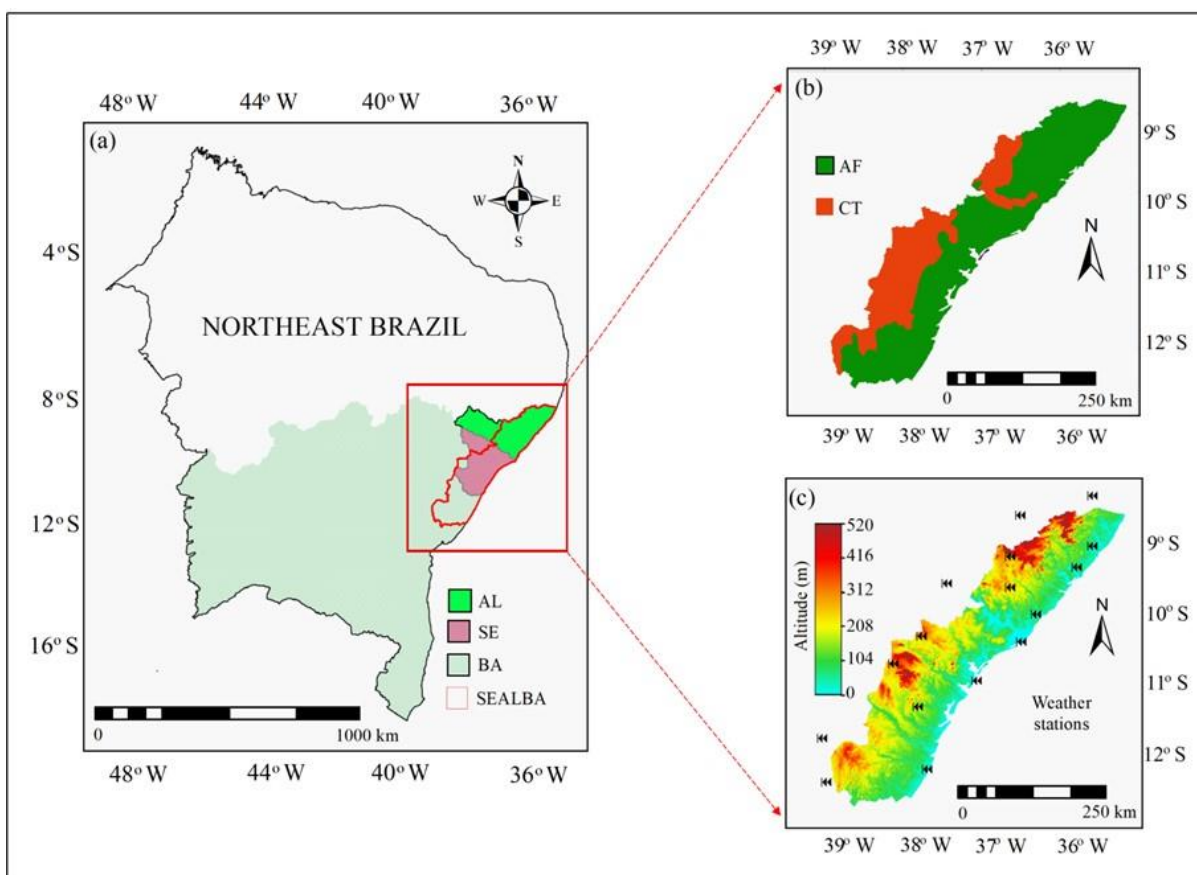


**Figure 1.** Location of the SEALBA agricultural growing region in Northeast Brazil, involving the states of Sergipe - SE, Alagoas - AL, and Bahia - BA (Figure 1a); the biomes within the region (Figure 1b); and altitudes together with the weather stations (Figure 1c).

Considering the MODIS pixel size of 250 m, 33% of SEALBA is in Sergipe - SE (2.0 Mha), 37% is in Alagoas - AL (2.3 Mha), and 30% is in Bahia - BA (1.9 Mha), totaling 6.2 Mha (Figure 1a), involving the Atlantic Forest (AF) and Caatinga (CT) biomes (Figure 1b). The areas in AF, with 3.9 Mha accounted, mostly below 275 m of altitude, occupies 63% of the SEALBA, in a portion closer to the coastline. The areas in CT, with 2.3 Mha accounted, are located further to the west side, being the majority above 275 m of altitude, representing 37% of SEALBA (Figures 1b and 1c).

The AF biome is characterized by forest vegetation, involving dense and open rain forests, semi-deciduous season forests, and ecosystems associated with the coastal lowlands. The climate is tropical humid but contrasting with mixed microclimates involving natural and anthropized areas. The AF environmental conditions are affected by moist air masses coming from the Atlantic Ocean, promoting high both air temperature and air humidity together with well distributed rainfall throughout the year (Francisquini et al., 2020).

The CT biome has species composed of trees and bushes with characteristics that allow environmental adaptations. These species are under high air temperatures but at low air humidity levels, with some drought periods throughout the year, developing resilience with increasing aridity (Almagro et al., 2017).

Both biomes, within the SEALBA agricultural growing region, have been experiencing fast replacement of their natural vegetation by crops as grains, fruits, sugar cane, forestry, and pasture (Procópio et al., 2019).

The input weather data for the large-scale energy balance modelling were incident global solar radiation ( $R_G$ ); air temperature ( $T_a$ ), air relative humidity (RH), and wind speed ( $u$ ); for the calculation of reference evapotranspiration ( $ET_0$ ) and (Allen et al., 1998) and the latent heat fluxes -  $\lambda E$ , applying the SAFER (Simple Algorithm for Evapotranspiration Retrieving) algorithm (Teixeira et al. 2017a, b; 2021). Through a geographic information system (GIS), these data were layered with the remote sensing parameters, contributing to a better spatial characterization of the energy balance components.

The bands 1 and 2 from the MODIS sensor (MOD13Q1 reflectance product) were downloaded from the site of EARTHDATA App EEARS (<https://lpdaacsvc.cr.usgs.gov/appears/>) and used together with the weather stations from INMET. The MODIS MOD13Q1 reflectance product, has spatial and temporal resolutions of 250 m and 16 days, respectively, giving 23 free-cloud images in a year, which together with the gridded weather data, allowed to model the average dynamics of the energy balance components in a year taking the long-term period from 2007 to 2021, allowing to quantify anomalies for specific periods from 2018 to 2021, in the AF and CT biomes inside the SEALBA agricultural growing region.

### Large-scale energy balance modelling

All the regression coefficients of the SAFER's equations applied from 2007 to 2021, described in the next sections, were determined by simultaneous satellite and field measurements in Northeast Brazil, involving natural vegetation and irrigated crops under strong contrasting thermohydrological conditions (Teixeira, 2010; Teixeira et al., 2008).

After clipping the MODIS reflectance images for the SEALBA region, the Normalized Difference Vegetation Index (NDVI) was calculated and incorporated in the modelling steps as a surface cover and root-zone moisture remote-sensing indicator:

$$NDVI = \frac{\rho_2 - \rho_1}{\rho_2 + \rho_1} \quad (1)$$

where  $\rho_1$  e  $\rho_2$  are respectively the MODIS reflectance from bands 1 (red) and 2 (near infra-red).

The pixel values of the surface albedo ( $\alpha_0$ ) were acquired as:

$$\alpha_0 = a + b\rho_1 + c\rho_2 \quad (2)$$

where a, b, and c are regression coefficients, which in the Northeast of Brazil, were 0.08, 0.41, and 0.14, from simultaneous remote sensing and field measurements, involving distinct irrigated crops and natural vegetation, under strong contrasting hydrological conditions (Teixeira, 2010; Teixeira et al., 2008).

For estimation of the daily surface temperature ( $T_0$ ) pixel values, without the MODIS thermal bands, this was done considering the short and long-wave radiation balance components. The remote sensing parameters and weather data were combined, through the Stefan-Boltzmann principle for the emitted both atmosphere and surface radiations.

Net radiation ( $R_n$ ) was estimated through the Slob equation (De Bruin, 1987):

$$R_n = (1 - \alpha_0)R_G - a_L \tau_{sw} \quad (3)$$

where  $\tau_{sw}$  is the short-wave atmospheric transmissivity calculated as the ratio of the incident global solar radiation measured by pyranometers ( $R_G$ ) to that at the top of the atmosphere ( $R_{TOP}$ ) calculated by astronomic parameters, while  $a_L$  is a regression coefficient up scaled through to the mean air temperature ( $T_a$ ) pixel values.

$$a_L = a_T T_a + b_T \quad (4)$$

being  $a_T$  and  $b_T$  for the Northeast Brazil were found as 6.8 and -40, respectively (Teixeira, 2010; Teixeira et al., 2008).

The atmospheric emissivity ( $\epsilon_A$ ) was calculated according to Almeida et al. (2023):

$$\epsilon_A = a_A (\ln \tau_{sw})^{b_A} \quad (5)$$

where  $a_A$  and  $b_A$  are regression coefficients are 0.94 and 0.11, respectively, for the Brazilian Northeast region (Teixeira, 2010; Teixeira et al., 2008).

The surface emissivity ( $\epsilon_0$ ) was estimated according to Teixeira, 2010:

$$\epsilon_0 = a_0 \ln NDVI + b_0 \quad (6)$$

where  $a_0$  and  $b_0$  are regression coefficients, which were reported as 0.06 and 1.00 for the Northeast Brazil (Teixeira, 2010; Teixeira et al., 2008).

Following the physical principle of the Stefan-Boltzmann' low, for the emitted radiation from atmosphere and from the ground surfaces (Teixeira et al., 2021),  $T_0$  was estimated as:

$$T_0 = \frac{\sqrt[4]{R_G(1-\alpha_0) + \sigma \epsilon_a T_a^4 - R_n}}{\sigma \epsilon_0} \quad (7)$$

where  $\sigma = 5.67 \cdot 10^{-8} \text{ W m}^{-2} \text{ K}^{-4}$  is the Stefan-Boltzmann constant.

To estimate the latent heat flux ( $\lambda E$ ), the ratio of the actual (ET) to reference ( $ET_0$ ) evapotranspiration ( $ET_0$ ), was first modeled for the satellite overpass time (subscript sat):

$$\left( \frac{ET}{ET_0} \right)_{\text{sat}} = \exp \left[ a_{\text{sf}} + b_{\text{sf}} \left( \frac{T_0}{\alpha_0 \text{NDVI}} \right) \right] \quad (8)$$

where the regression coefficients  $a_{\text{sf}}$  and  $b_{\text{sf}}$  found for the Brazilian Northeast were 1.90 and -0.008 (Teixeira, 2010; Teixeira et al., 2008).

Eq. 8 does not work for water bodies or mixture of land and water ( $\text{NDVI} < 0$ ); thus, the concept of equilibrium evapotranspiration (Raupasch, 2001) is introduced in the SAFER algorithm for pixels under these conditions, with the equilibrium latent heat fluxes ( $\lambda E_{\text{eq}}$ ), at daily timescale, considered as:

$$\lambda E_{\text{eq}} = \left( \frac{\Delta (R_n - G)}{\Delta + \gamma} \right) \quad (9)$$

where  $\Delta$  is the slope of the curve relating the saturation vapor pressure ( $e_s$ ) and  $T_a$ ,  $\gamma$  is the psychrometric constant, and  $G$  is the ground heat fluxes estimated according to Teixeira (2010):

$$G = [a_G \exp(b_G \alpha_0)] R_n \quad (10)$$

being  $a_G$  and  $b_G$  regression coefficients, found to be 3.98 and -25.47, respectively, for the Northeast Brazil (Teixeira, 2010; Teixeira et al., 2008).

Considering that the satellite overpass values of the  $ET/ET_0$  fraction does not differ so much from the daily ones (Allen et al. 2007), throughout conditional functions applied to the NDVI values, the daily  $\lambda E$  pixel values were estimated considering the daily averages of the calculated reference evapotranspiration from the net of weather stations ( $ET_{0-24}$ )

$$\lambda E = 2.45 \left( \frac{ET}{ET_0} \right)_{\text{sat}} ET_{0-24} \text{ or } \lambda E_{\text{eq}} \quad (11)$$

being  $ET_{0-24}$  calculated by using the gridded daily weather data on  $R_G$ ,  $T_a$ , RH, and  $u$  (Allen et al., 1998) and 2.45 a unit conversion factor.

To close the simplified energy balance equation, the sensitive heat flux (H) was estimated as a residue, having recovered all the other energy balance components (Teixeira et al., 2017a, b, 2021):

$$H = R_n - \lambda E - G \quad (12)$$

To infer the root-zone moisture conditions, the evaporative fraction (Ef) was estimated as:

$$Ef = \frac{\lambda E}{R_n - G} \quad (13)$$

All the energy balance analyzes were done for the SEALBA region, classifying the biomes Atlantic Forest (AF) and Caatinga (CT), to consider the behaviors of their different agroecosystems under varying environmental conditions over the years studied.

## RESULTADOS E DISCUSSÃO

### RESULTS AND DISCUSSION

#### Long-term weather drivers

As for the energy balance partitions the main weather drivers are precipitation (P) and incident solar global radiation ( $R_G$ ), to characterize the average environmental conditions, Figure 2 shows their long-term average pixel values from 2007 to 2021, and standard deviations (SD), for the Atlantic Forest (AF) and Caatinga (CT) within SEALBA, at the MODIS reflectance 16-day timescale, in terms of Day of the Year (DOY).

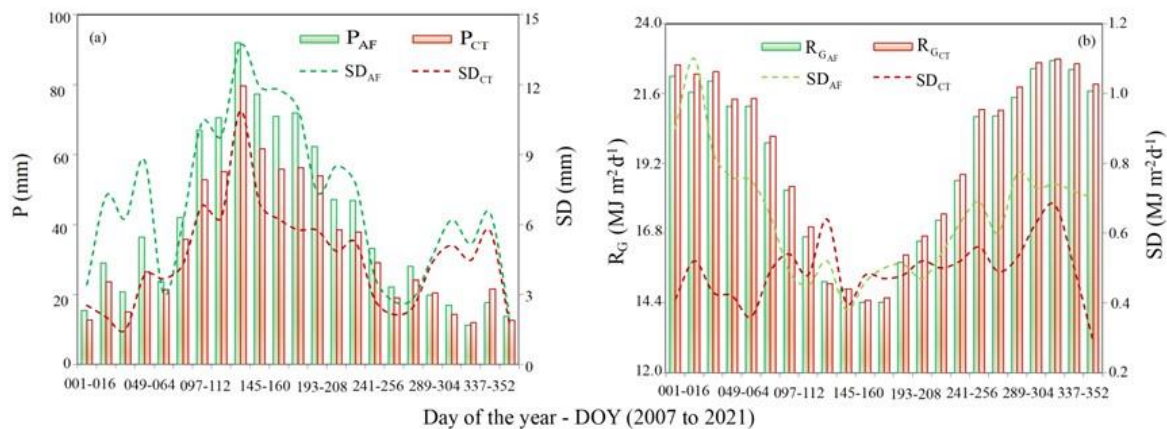


**Figure 2.** Average pixel values and standard deviations (SD) for precipitation - P (a) and global solar radiation -  $R_G$  (b), at the MODIS reflectance 16-day timescale, for the Atlantic Forest (AF) and Caatinga (CT) biomes, within the SEALBA agricultural growing region, in terms of Day of the Year (DOY), regarding the period 2007 to 2021.

From Figure 2a, rainfall is concentrated in the middle of the year for both biomes, AF and CT, with the high amounts for the first one. The highest P pixel values occur from April to July (DOY 097-208), when the 16-day average totals are above 60 mm for AF, and higher than 50 mm for CT. The lowest ones, with totals below 15 mm for both biomes, are from November to January (DOY 305-

016), which limit water fluxes from surfaces to the lower atmosphere. Regarding the annual scale, the mean total in CT, accounting  $780 \text{ mm yr}^{-1}$ , is 83% of that for AF ( $936 \text{ mm yr}^{-1}$ ). The largest spatial variations between biomes are for AF, where the SD values represent 17% of the annual P, while for CT the corresponding percentage is 14%.

The  $R_G$  average values show an inverse tendency along the year when compared with that for P. The highest  $R_G$  levels are from October to March (DOY 289-065), with averages above  $21.0 \text{ MJ m}^{-2} \text{ d}^{-1}$  for both biomes, which together with lower rainfall amounts are in favor for warmer conditions. The lowest  $R_G$  rates happen at the middle of the year in June (DOY 161-176), when dropped to below  $14.5 \text{ MJ m}^{-2} \text{ d}^{-1}$ . However, much lower differences on  $R_G$  values arise between AF and CT when comparing to the P ranges, with the average  $R_G$  for AF being 99% of that for CT. Similar  $R_G$  spatial variations between biomes are detected in the middle of the year, when SD accounts only for 3% of the average pixel values, but the highest SD occur in AF outside this period, mainly at the start of the year, when it represents 4-5% of the average values against 2% for CT.

Drops in precipitation together with increasing solar radiation levels at the start and at the end of the year in SEALBA contribute for depletion of root-zone moisture through  $\lambda E$ , promoting reduction of vegetation activity, and then, increasing H rates (Sun et al., 2015).

### 3.2. Long-term energy balance

Figure 3 presents the average pixel values and standard deviations (SD) for net radiation -  $R_n$  (Figure 3a) and its partition into latent -  $\lambda E$  (Figure 3b), sensible - H (Figure 3c), and ground - G (Figure 3c) heat fluxes, at the MODIS 16-day timescale, for the long-term period from 2007 to 2021 in terms of Day of the Year (DOY). Data are classified for the Atlantic Forest (AF) and Caatinga (CT) biomes, within the SEALBA agricultural growing region.

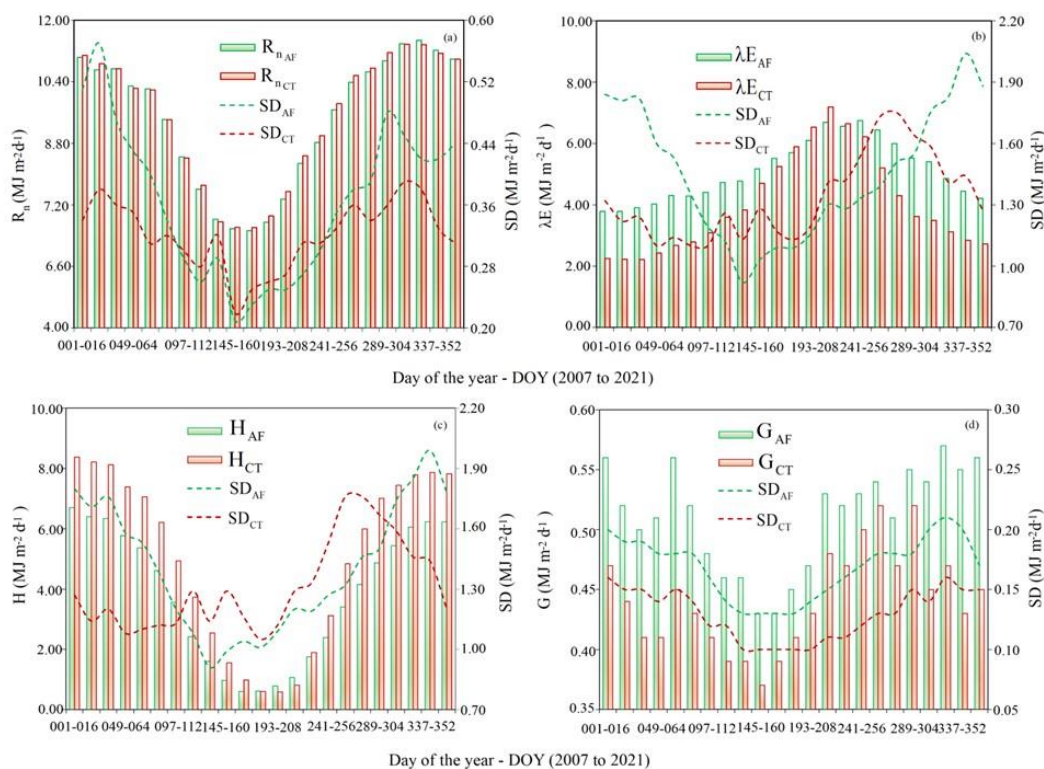


Figure 3. Average values and standard deviations (SD), of the energy balance components at the 16-day MODIS timescale in terms of Day of the Year (DOY), for the long-term period from 2007 to 2021. Data are classified for the Atlantic Forest (AF) and Caatinga (CT) biomes, within the SEALBA



agricultural growing region. (a) net radiation -  $R_n$ ; (b) latent heat flux -  $\lambda E$ ; (c) sensible heat flux -  $H$ ; (d) ground heat flux -  $G$ .

The  $R_n$  values follow those for  $R_G$  (Figure 3a), ranging from 6.50 to 11.50  $\text{MJ m}^{-2} \text{d}^{-1}$ , with the highest averages at the start and at the end of the year, while the lowest ones at the middle of the year, for both AF and CT, however slightly higher for the second biome. At the annual scale, the  $R_n$  rates in AF were 99% of those for CT, with the largest spatial variations for the first biome at the start of the year, according to the SD values. Crossing Figures 2b and 3a, the ratio  $R_n/R_G$  ranges from 0.44 from May to June (DOY 145-160) to 0.52 from August to September (DOY 241-256). During this last period occur conditions of higher available energy, at the end of the rainy season, when the root-zones are still under good moisture conditions, favorable for  $\lambda E$ .

From energy balance measurements from 2011 to 2012 in AF within the Brazilian Southeast region, Funari and Filho (2014) found daily  $R_n$  between 4.00 to 15.00  $\text{MJ m}^{-2} \text{d}^{-1}$  from May to December, yielding  $R_n/R_G$  values from 0.40 to 0.68. Through Landsat measurements in CT within Northeast Brazil, Teixeira et al. (2017a) reported  $R_n$  values from 8.90 to 11.40  $\text{MJ m}^{-2} \text{d}^{-1}$ , resulting in a  $R_n/R_G$  ratio range from 0.41 to 0.47. These previous results for both AF and CT biomes, are inside of our results.

Regarding the  $R_n$  partition into  $\lambda E$ , stronger differences between the AF and CT biomes arise (Figure 3b). The largest  $\lambda E$  rates are for AF at the start and at the end of the year, outside the rainy periods (see also Figure 2a). The average  $\lambda E$  along the year is between 3.80 and 6.80  $\text{MJ m}^{-2} \text{d}^{-1}$  for AF and from 2.20 to 7.20  $\text{MJ m}^{-2} \text{d}^{-1}$  for CT, with average annual values of 5.10  $\text{MJ m}^{-2} \text{d}^{-1}$  and 4.00  $\text{MJ m}^{-2} \text{d}^{-1}$ , respectively, being the rates for AF 26% higher than those for CT. However, from June (DOY 177) to August (DOY 224), the end the rainy season, the CT species present larger  $\lambda E$  rates than those for AF, period when the root-zone moisture is not limited for both biomes. The highest  $\lambda E$  spatial variations happen at the start (January to March, DOY 001-064) and at the end (November to December, DOY 305-352) of the year, in both biomes, when the SD values surpass 50% of the average pixel values. At the annual scale SD represents 33% of the average  $\lambda E$  for CT, while this percentage is 28% for AF. The annual  $\lambda E/R_n$  values were 0.54 and 0.43 for AF and CT, respectively, however, inside the rainy period this ratio is higher than 0.80 for both biomes, indicated the best root-zone moisture conditions for rainfed agriculture, while outside this period this ratio falls to 34% and 20% for AF and CT, respectively, meaning higher water stress conditions for CT and irrigation needs for agricultural crops.

Applying the water balance method in remnant AF after a prolonged drought, Rodrigues et al. (2021) reported an ET range corresponding to  $\lambda E$  values from 3.43 to 4.42  $\text{MJ m}^{-2} \text{d}^{-1}$ , like our detected values for the driest conditions for this biome at the start and at the end of the year. From micrometeorological measurements in AF, Guauque-Mellado et al. (2022) reported higher  $\lambda E/R_n$  values from 0.86 to 0.88, but the authors neglected the fraction of  $R_n$  partitioned into  $G$ . However, also from micrometeorological measurements in AF, Funari and Filho (2014) found daily  $\lambda E/R_n$  values between 0.47 to 0.65, inside our range. From energy balance measurements in CT, Silva et al. (2017) found average  $\lambda E$  ranging from 2.40  $\text{MJ m}^{-2} \text{d}^{-1}$ , during the dry period, to 4.80  $\text{MJ m}^{-2} \text{d}^{-1}$  inside the rainy season, yielding respective  $\lambda E/R_n$  values of 0.23 to 0.41. Campos et al. (2019), also applying the same techniques in CT, reported  $\lambda E/R_n$  annual values of 0.20, like our ranges for this biome. However, from microclimate measurements in CT, Marques et al. (2020) reported average  $\lambda E$  values between 0.49 and 0.74  $\text{MJ m}^{-2} \text{d}^{-1}$  under the driest conditions till a range from 4.17 to 6.37  $\text{MJ m}^{-2} \text{d}^{-1}$ , during the rainy season. The higher values from this last previous study represent good root-zone moisture conditions, like our values during the rainy period, however their lower end values are lower, as their study was carried out in drier semiarid areas, more to the west side of the CT biome.

The highest  $H$  are at the start and at the end of the year for both biomes, AF and CT (Figure 3c), with average pixel values above 6.00  $\text{MJ m}^{-2} \text{d}^{-1}$  in AF and higher than 8.00  $\text{MJ m}^{-2} \text{d}^{-1}$  in CT, from January

to February (DOY 001-048). High H at low P (see also Figure 2a), lead to a reduction of available water resources (Huang et al., 2017; Yang et al., 2016). The lowest H rates, with averages below  $1.00 \text{ MJ m}^{-2} \text{ d}^{-1}$  occur during the rainy season, in the middle of the year, from June to July (DOY 161-208). Although in general CT presents higher H values than those for AF, there is a short period when they are slightly lower, from June to August (DOY 177-224). At the annual scale CT presents a daily average H of  $5.00 \text{ MJ m}^{-2} \text{ d}^{-1}$ , 32% higher than that for AF ( $3.80 \text{ MJ m}^{-2} \text{ d}^{-1}$ ). More H spatial variations happen in AF than in CT, with SD representing 37 e 26% of the average values, respectively, at the annual scale. Inside the rainy period the H/R<sub>n</sub> ratio drops to below 0.20 in both biomes, indicated good conditions for rainfed agriculture, while outside this period, at the start and at the end of the year, this ratio is above 0.55 and 0.75 for AF and CT, respectively, meaning higher warming and water stress conditions for CT.

From field energy balance measurements in AF inside the Brazilian Southeast region, Guauque-Mellado et al. (2022) reported H/R<sub>n</sub> ranging from 12 to 14%, much lower than our ratios in Northeast Brazil. However, also from micrometeorological measurements in AF inside in the same region, Funari and Filho (2014) found daily H rates between  $1.10$  to  $6.90 \text{ MJ m}^{-2} \text{ d}^{-1}$ , from May to December, yielding H/R<sub>n</sub> values from 0.25 to 0.42, inside our ranges. The H values for CT in the current study are larger than those reported by Teixeira et al. (2021) from Landsat measurements in irrigated lemon crop in CT, who found annual averages of  $2.82 \text{ MJ m}^{-2} \text{ d}^{-1}$ ,  $1.53 \text{ MJ m}^{-2} \text{ d}^{-1}$ , and  $0.19 \text{ MJ m}^{-2} \text{ d}^{-1}$  under drip, micro sprinkler, and pivot irrigation systems, respectively. These last lower values can be explained by the frequent occurrence of heat advection from the hotter areas at the vicinities of irrigated plots (Console and Papa, 2013). However, Campos et al. (2019), also from energy balance measurements in CT, reported H/R<sub>n</sub> annual values of 0.50, like our average value of 0.53.

Among the energy balance components in the SEALBA agricultural growing region, G is the lowest one (Figure 3d). Although its amplitude is not large, there are differences between the biomes, being the minimum average values  $0.43$  and  $0.37 \text{ MJ m}^{-2} \text{ d}^{-1}$  for AF and CT, respectively, happening from May to June (DOY 145-160), while the corresponding maximums are  $0.57 \text{ MJ m}^{-2} \text{ d}^{-1}$  in AF, from November to December (DOY 321-336) and  $0.52 \text{ MJ m}^{-2} \text{ d}^{-1}$  in CT, from October to November (DOY 289-304). At the annual scale, the average G in AF is 16% higher than that for CT. The SD values for AF represent 33% of the mean pixel value, while for CT this percentage is 29%. The lower G rates for CT may be explained by the fact that being at daily scales, and as the soil cover is lower than for AF, much long wave radiation is emitted at night, similarly to deserts. Regarding the G/R<sub>n</sub> ratio, it was very small for both biomes, ranging from 0.04 to 0.07, with this high end being for the AF biome.

From energy balance measurements in AF inside the Brazilian Southeast region, Funari and Filho (2014) found daily G values between  $0.30$  to  $2.40 \text{ MJ m}^{-2} \text{ d}^{-1}$  from May to December, yielding G/R<sub>n</sub> from 0.03 to 0.24. The high end of this range is much larger than our ones for AF, but their rates involved urban areas of the big São Paulo city. However, Silva et al. (2017) reported average G values of  $0.33$  and  $0.35 \text{ MJ m}^{-2} \text{ d}^{-1}$  for the dry and wet seasons for CT in the Brazilian Northeast, yielding an average low G/R<sub>n</sub> value of 0.03. Under dry and wet conditions in CT, Campos et al. (2019) measured G ranging from  $-0.80$  to  $6.50 \text{ MJ m}^{-2} \text{ d}^{-1}$ , with corresponding G/R<sub>n</sub> values between  $-0.04$  to  $0.04$ . The negative values, at shorter timescales, mean heat advection from the warmer vicinities of the measured area (Teixeira et al., 2021).

Having the pixel values for  $\lambda E$  and the available energy ( $R_n - G$ ),  $E_f$  was calculated classifying the biomes AF and CT (Eq. 13) and considered representative of the root-zone moisture conditions. The long-term annual  $E_f$  values (2007-2021) were 0.60 for AF and 0.48 for CT, being the highest values in 2020, when the average for the SEALBA agricultural growing region was 0.62, while the lowest ones happened in driest year 2018, when it was 0.48.

To have an idea of a large-scale energy balance monitoring system, Figure 4 shows the spatial distributions, averages, and standard deviations (SD) of the annual evaporative fraction (Ef) values for the last four years of the data set (2018, 2019, 2020, and 2021), classifying the Atlantic Forest (AF) and Caatinga (CT) within the SEALBA agricultural growing region.

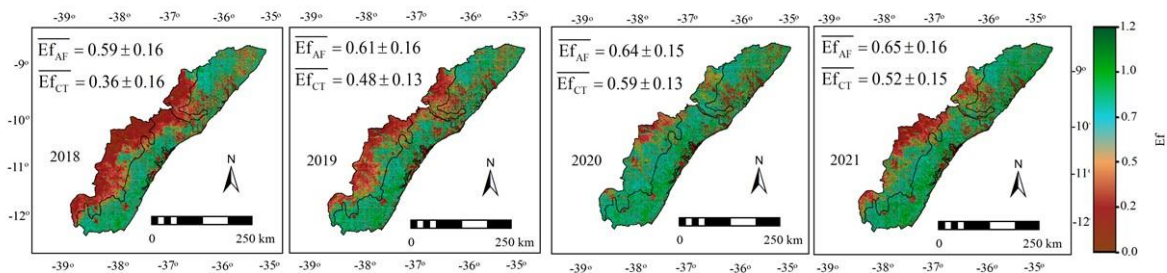


**Figure 4.** Spatial distributions, averages, and standard deviations of the annual pixel values for the evaporative fraction (Ef), regarding the last four years of the data set (2018, 2019, 2020, and 2021), classifying the Atlantic Forest (AF) and Caatinga (CT) biomes within the SEALBA agricultural growing region.

Following Figure 4, the root-zone moisture levels were extremely variable along the year from 2018 to 2021, with the Ef values for AF were 8% to 64% larger than those for CT, being the highest values for both biomes in the wettest year of 2021, when the average for the SEALBA agricultural growing region was 0.62, while the lowest ones happened in driest year 2018, when it was 0.48. These mean Ef pixel values indicated good root-zone moisture for rainfed agriculture from 2019 to 2021, mainly for the AF biome, as they were above 0.60.

Increasing Ef means higher root-zone moisture levels for vegetation (Teixeira et al., 2021), while lower ones identify water stress (Lu et al., 2011). According to Yuan et al. (2016), these effects reducing vegetation growth, are related to low root-zone moisture conditions, but also biomass production depends also on the available energy (Zhang et al., 2021). Zhou and Zhou (2009), reported that air humidity and the available energy, were the most important variables for the root-zone moisture variations in a reed marsh in Northeast China. However, Ef values in plants under non-optimum moisture levels, are also influenced by the stomatal regulation (Mateos et al., 2013), mechanism much noticed for the CT species.

It is concluded that latent and sensible fluxes, and then the root-zone moisture conditions, may strongly vary among years and seasons, for both Brazilian biomes inside the SEALBA agricultural growing region. However, water availability to the root zones is higher for AF than that for CT, as changes in vegetation canopies strongly vary between their species, according to environmental conditions, and canopy changes are higher in CT than in AF during water stress events.

Overall, the energy balance modelling with the MOD13Q1 reflectance product, can be used to investigate the anomalies on the water availability conditions along the years in distinct biomes. These analyzes are important for water policies as they may show suitable periods and places for rainfed agriculture as well as the irrigation needs for irrigated agriculture along specific seasons of a year, allowing rational agricultural water management while helping to minimize competitions among other water users.

These long-term energy balance analyses are important for environmental policies because they picture the patterns of the energy fluxes among distinct biomes within the agricultural growing region of SEALBA. From the  $R_n$  average pixel values, one can know the available energy to the surfaces, while quantifying its average partitions into  $\lambda E$ ,  $H$ , and  $G$  allow to support natural resources

management and to create rational criteria for managements of rainfed and irrigated agricultural, while helping to minimize competitions among other water users.

## CONCLUSÃO

### CONCLUSION

We confirmed the suitability of applying the SAFER algorithm through the union of MODIS images and net of agrometeorological stations for large-scale monitoring of energy and water balance components and their anomalies using long series of satellite images and weather data for distinct biomes, under conditions of climate and land-use changes. Our specific analyzes involved the Atlantic Forest (AF) and Caatinga (CT) biomes within the coastal agricultural growing zone in the Northeast Brazil, limited by the states of Sergipe (SE), Alagoas (AL), and Bahia (BA), acronym for SEALBA.

In both SEALBA biomes, net radiation ( $R_n$ ) values follow the solar radiation levels, with the highest rates at the start and at the end of the year, while the lowest ones are at the middle of the year, however slightly higher for CT than for AF. However, significant differences on partitions of the net radiation ( $R_n$ ) into latent ( $\lambda E$ ), sensible (H), and ground (G) fluxes between the biomes, promoted distinct root-zone moisture conditions, represented by the evaporative fraction ( $E_f$ ).

The largest  $\lambda E$  and lowest H values are for AF at the start and at the end of the year, outside the rainy periods, being the  $\lambda E$  rates for AF 26% higher than those for CT, while for H the values for CT were 32% above those for AF, at the annual scale. Among the energy balance components, G is the lowest one, however, being the values in AF 16% above those for CT. The lower G for CT may be explained by the fact that being at daily scales, and as its soil cover is lower than that for AF, much long wave radiation from their species is emitted at night, similarly to deserts. Energy balance computations yielded  $E_f$  values higher for AF than for CT, evidencing moister root-zone conditions for the first biome.

These energy and water balance assessments being carried out year after year, throughout a monitoring system, may support water policies as they picture suitable periods and places for rainfed agriculture as well as the irrigation needs for irrigated agriculture, allowing rational agricultural water management while minimizing water competitions among other water users.

## AGRADECIMENTOS

### ACKNOWLEDGEMENTS

To the National Council for Scientific and Technological Development (CNPq), for funding the project "Monitoring the balances of energy, water, and carbon, with geotechnologies in the SEALBA region, grant number 311532/2021-7

## REFERÊNCIAS

### REFERENCES

Allen, RG, Pereira, LS, Raes, D., Smith, M. Crop evapotranspiration, Guidelines for computing crop water requirements, FAO Irrigation and Drainage Paper 56. Rome, Italy, 300 pp., 1998.

Almagro, A.; Oliveira, PTS; Nearing, MA Projected climate change impacts in rainfall erosivity over Brazil. **Scientific Reports** , vol. 7, 8130, 2017.

- Almeida, SLH de, Souza, JBC, Pilon, C., Teixeira, AH de C., Santos, AF dos, Sysskind, MN, Vellidis, G., Silva, RP da., 2023. Performance of the SAFER model in estimation peanut maturation. **European Journal of Agronomy** , vol. 147, 126844, 2023.
- Campos, S., Mendes, KR, Silva, LL da, Mutti, PR, Medeiros, SS, Amorim, LB, Santos, CAC dos, Perez-Marin, AM, Ramos, TM, Marques, TV, Lucio, PS, Costa , GB, Santos e Silva, CM, Bezerra, BG. Closure and partitioning of the energy balance in a preserved area of ??a Brazilian seasonally dry tropical forest. **Agricultural and Forest Meteorology** , vol. 271, 398-412, 2019.
- Consoli, S., Papa, R. Corrected surface energy balance to measure and model the evapotranspiration of irrigated orange orchards in semi-arid Mediterranean conditions. **Irrigation Science** , vol. 31, 1159-1171, 2013.
- Consoli, S., Vanella, D. Comparisons of satellite-based models for estimating evapotranspiration fluxes. **Journal of Hydrology** , vol. 513, 475-489, 2014.
- De Bruin HAR From Penman to Makkink, in: Hooghart, JC (Ed.), Proceedings and Information: TNO Committee on Hydrological Sciences, v. 39. Gravenhage, The Netherlands, pp. 5-31, 1987.
- Francisquini, MI, Lorente, FL, Pessenda, LCR, Junior, AAB, Mayle, FE., Cohen, MCL, França, MC, Bendassolli, JA, Giannini, PCF, Schiavo, JA, Macario, K. Cold and humid Atlantic Rainforest during the last glacial maximum, northern Espírito Santo state, southeastern Brazil. **Quarterly Science Review** , vol. 244, 106489, 2020.
- Funari, FL, Filho, AJP Energy balance in a patch of the Atlantic Forest in São Paulo City, Brazil. **Journal of Water Resources** , vol. 6, 805-812, 2014.
- Guauque-Melado, D., Rodrigues, A., Terra, M., Yanagi, S., Diotto, A.; de Mello, C. Evapotranspiration under drought conditions: the case study of a seasonally dry Atlantic Forest. **Atmosphere** , vol. 13, 871, 2022.
- Lewinsohn, T. M.; Prado, PI How many species are there in Brazil? **Conservation Biology** , vol. 19, 619-624, 2005.
- Lu, N., Chen, S., Wilske, B., Sun, G., Chen, J. Evapotranspiration and soil water relationships in a range of disturbed and undisturbed ecosystems in the semiarid Inner Mongolia, China. **Journal of Plant Ecology** , vol. 4, 49-60, 2011.
- Mariano, D. A.; Santos, C. A. C. dos; Wardlowa, B. D.; Anderson, M. C.; Schiltmeyera, A. V.; Tadessea, T.; Svoboda, M. D. Use of remote sensing indicators to assess effects of drought and human induced land degradation on ecosystem health in Northeastern Brazil. **Remote Sensing of Environment**, v. 213, 129-143, 2018.
- Marques, T.V., Mendes, K, Mutti. P., Medeiros, S., Silva, L., Perez-Marin, A.M., Campos, S., Lúcio, P.S., Lima, K., Reis, J. dos, Ramos, T.M., Silva, D.F. da, Oliveira, C.P., Costa, G.B., Antonino, A.C.D., Menezes, R.S.C., Santos e Silva, C.M., Bergson, B. Environmental and biophysical controls of evapotranspiration from seasonally dry tropical forests (Caatinga) in the Brazilian Semiarid. **Agricultural and Forest Meteorology**, v. 287, 107957, 2020.
- Mateos, L., González-Dugo, M.P., Testi, L., Villalobos, F.J. Monitoring evapotranspiration of irrigated crops using crop coefficients derived from time series of satellite images. I. Method validation. **Agricultural Water Management**, v. 125, 81-91, 2013.

- Pereira, D.R, Mello, C.R. de, Silva, A.M. da, Yanagi, S.N.M. Evapotranspiration and estimation of aerodynamic and stomatal conductance in a fragment of Atlantic Forest in Mantiqueira range region, MG. **Cerne**, v. 16, 32-40, 2010.
- Procopio, S. de O, Cruz, M.A.S., Almeida, M.R.M. de, Jesus Junior, L.A. de, Nogueira Junior, L.R., Carvalho, H.W.L. de. SEALBA: região de alto potencial agrícola no Nordeste brasileiro. Aracaju: Embrapa Tabuleiros Costeiros, 2019. (Embrapa Tabuleiros Costeiros, Documentos, 221), 2019.
- Raupasch, M.R. Combination theory and equilibrium evaporation. **Quarterly Journal of the Royal Meteorological Society**, v. 127, 1149-1181, 2001.
- Rodrigues, A.F., Mello, C.R. de, Terra, M.C.N.S., Beskow, S. Water balance of an Atlantic Forest remnant under a prolonged drought period. **Ciência e Agrotecnologia**, v. 45, e008421, 2021.
- Silva, P. F. da, Lima, J. R. de S., Antonino, A. C. D., Souza, R., Souza, E. S. de, Silva, J. R. I., Alves, E. M. Seasonal patterns of carbon dioxide, water, and energy fluxes over the Caatinga and grassland in the semi-arid region of Brazil. **Journal of Arid Environments**, v. 147, 71-82, 2017.
- Sun, Y., Fu, R., Dickinson, R., Joiner, J., Frankenberg, C., Gu, L., Xia, Y., Fernando, N. Drought onset mechanisms revealed by satellite solar-induced chlorophyll fluorescence: Insights from two contrasting extreme events. **Journal of Geophysical Research: Biogeosciences**, v. 120, 2427-2440, 2015.
- Teixeira, A. H. de C. Determining regional actual evapotranspiration of irrigated and natural vegetation in the São Francisco River basin (Brazil) using remote sensing and Penman-Monteith equation. **Remote Sensing**, v. 2, 1287-1319, 2010.
- Teixeira, AH de C.; Bastiaanssen, WGM; Ahmad, MD; Moura, MSB; Bos, MG Analysis of energy fluxes and vegetation-atmosphere parameters in irrigated and natural ecosystems of semi-arid Brazil. **Journal of Hydrology** , vol. 362, 110-127, 2008.
- Teixeira, AH, de C, Leivas, JF, Hernandez, FBT, Franco, RAM Large-scale radiation and energy balances with Landsat 8 images and agrometeorological data in the Brazilian semiarid region. **Journal of Applied Remote Sensing** , vol. 11, 016030, 2017a.
- Teixeira, AH, de C, Leivas, JF, Ronquim, CC, Silva, GB The Use of MODIS Images to Quantify the Energy Balance in Different Agroecosystems in Brazil. In: Rustamov, RB, Hasanova, S., Zeylanova, MH (Eds.). **Multi-purposeful application of geospatial data** ( 1 ed., pp. 105-121) IntechOpen Limited, London, 2017.
- Teixeira, AH de C.; Leivas, JF; Struiving, TB; Reis, JBRS; Simão, FR Energy balance and irrigation performance assessments in lemon orchards by applying the SAFER algorithm to Landsat 8 images. **Agricultural Water Management** , vol. 247, 1- 9, 2021.
- Yuan, W., Cai, W., Chen, Y., Liu, S., Dong, W., Zhang, H., Yu, G., Chen, Z., He, H., Guo, W., Liu, D., Liu, S., Xiang, W., Xie, Z., Zhao, Z., Zhou, G. Severe summer heatwave and drought strongly reduced carbon uptake in Southern China. **Science Reports** , vol. 6, 18813, 2016.
- Zhang, G., Su, X., Singh, VP, Ayantobo, O. Appraising standardized moisture anomaly index (SZI) in drought projection across China under CMIP6 forcing scenarios. **Journal of Hydrology: Regional Studies** , vol. 37, 100898, 2021.

Zhou, L.; Zhou, G. Measurement and modeling of evapotranspiration over a reed (*Phragmites australis*) marsh in Northeast China. **Journal of Hydrology** , vol. 372, 41-47, 2009.